

LOCALIZED FAILURE ASSESSMENT IN RECYCLED AGGREGATE CONCRETE

Sonia M. Vrech^{a,b}, Marianela Ripani^{a,c} and Guillermo Etse^{a,b,c}

^a*CONICET, National Scientific and Technical Research Council, Argentina.*

^b*CEMNCI, Faculty of Exact Sciences and Engineering, National University of Tucuman, Argentina.*

^c*LMNI, Faculty of Engineering, University of Buenos Aires, Argentina.*

Keywords: Discontinuous bifurcation, recycled aggregate concrete, gradient plasticity.

Abstract. In this work, the discontinuous bifurcation condition is evaluated for Recycled Aggregate Concretes (RAC) in limit states by means of the description of the localization indicator, based on the acoustic or localization tensor. This is performed in the framework of a thermodynamically consistent non-local plasticity for quasi-brittle materials like concrete, based on gradient plasticity and fracture energy homogenization. Explicit solutions for brittle failure conditions are proposed in the form of discontinuous bifurcation and they provide relevant information regarding the variation of the transition point of brittle-ductile failure modes with the recycled aggregate content and confining pressure. Finally, numerical results demonstrate the performance of the localization indicator for different confinement pressures and recycled aggregate contents.

1 INTRODUCTION

The construction sector is one of the most energy consuming (NRMCA (2012)). In this context, the use of recycled aggregates in the fabrication of concrete offers a very interesting technique to reduce energy consume and contamination. Several building codes (RILEM-TC-121-DRG (1994); NTC (2008)) have reflected the knowledge improvements made by the international scientific community on the mechanical behavior of RAC.

Experimental contributions by Kou and Poon (2012); Lima et al. (2013); Folino and Xargay (2014) have demonstrated that even though some relevant mechanical properties of RAC such as compressive and tensile strengths and its elasticity modulus may be lower than those of Natural Aggregate Concrete (NAC), the overall mechanical behavior of RAC is still appropriated for structural use. Numerical constitutive formulations are mainly oriented to predict the uniaxial compression stress-strain behavior (see a.o. Du et al. (2010); Li et al. (2010)).

In this paper, the localized failure assessment in RAC is performed, based on the so-called Leon-Drucker Prager (LDP) constitutive model by Etse et al. (2016). The localization tensor is formulated and its performance in the form of discontinuous bifurcation is numerically evaluated. The obtained results demonstrate the capabilities of the proposed model to reproduce failure behaviors of RAC under arbitrary stress states and recycled aggregate contents. The localization analyses demonstrate, particularly in plane stress conditions, that the addition of recycled aggregated does strongly increase the potentials for discontinuous failure modes. Moreover, it is demonstrated that the effect of the recycled aggregated content on the failure mode for localized failure is much less significant in case of plane strain conditions.

2 THERMODYNAMICS OF GRADIENT-BASED POROPLASTIC MATERIALS

In this section the Thermodynamics laws are considered to formulate and derive the thermodynamically consistent expressions of the constitutive equations for gradient-based poroplastic continua as considered for the modeling of RAC (see Etse et al. (2016)). Based on the original proposal by Simo and Miehe (1992) for local inelastic media and its extension for gradient plasticity and small strain kinematics by Svedberg and Runesson (1997) and Vrech and Etse (2009), arbitrary thermodynamic states of thermodynamically consistent gradient-regularized materials may be defined in terms of the elastic strain tensor $\boldsymbol{\varepsilon}^e = \boldsymbol{\varepsilon} - \boldsymbol{\varepsilon}^p$, the elastic entropy $s^e = s - s^p$, the internal variable q and their spatial gradients ∇q . Therefore, the internal energy density can be expressed as

$$e = e(\boldsymbol{\varepsilon}^e, s^e, q, \nabla q). \quad (1)$$

Under consideration of the decomposition of the free energy density in the form $\psi = e - Ts$, being T the absolute temperature and the Clausius-Duhem inequality, the Coleman's equations, the local and gradient dissipative stresses and the plastic, thermal and boundary dissipations can be expressed in terms of ψ , as follows

$$\boldsymbol{\sigma} = \rho \frac{\partial \psi}{\partial \boldsymbol{\varepsilon}^e} \quad ; \quad s = -\frac{\partial \psi}{\partial T} \quad (2)$$

$$Q_R = -\rho \frac{\partial \psi}{\partial q} \quad ; \quad Q^g = T \nabla \cdot \left(\frac{\rho}{T} \frac{\partial \psi}{\partial \nabla q} \right) \quad (3)$$

$$\varphi^p = \boldsymbol{\sigma} : \dot{\boldsymbol{\varepsilon}}^p + Q_R \dot{q} \quad ; \quad \varphi^{th} = -\frac{\mathbf{h} \cdot \nabla T}{T} \quad (4)$$

$$\varphi^{(b)} = \int_{\partial\Omega} Q^{(b)} \dot{q} \, d\partial\Omega \quad \text{with} \quad Q^{(b)} = -\mathbf{n}_s \cdot \rho \frac{\partial\psi}{\partial\nabla q} \quad (5)$$

being \mathbf{h} the heat flux vector and \mathbf{n}_s the normal to the boundary. Note that Q_R indicates the dependency of the dissipative stresses on the recycled aggregate content. The following uncoupled expression of the total Helmholtz's free energy density is adopted for gradient-based elastoplastic materials

$$\psi(\boldsymbol{\varepsilon}^e, q, \nabla q) = \psi^e(\boldsymbol{\varepsilon}^e) + \psi^l(q) + \psi^g(\nabla q) \quad (6)$$

Assuming the following expressions for the elastic, local and non-local plastic free energy

$$\rho\psi^e = \frac{1}{2} \boldsymbol{\varepsilon}^e : \mathbf{C} : \boldsymbol{\varepsilon}^e, \quad (7)$$

$$\rho\psi^l = \frac{H^l}{2} q^2, \quad (8)$$

$$\rho\psi^g = \frac{1}{2} l_c^2 H^g \nabla \cdot \nabla q, \quad (9)$$

being \mathbf{C} the fourth order elastic tensor, H^l the local-plastic hardening/softening modulus, H^g the gradient softening modulus and l_c the gradient characteristic length; the corresponding Cauchy tensor, local and non-local dissipative stresses result

$$\boldsymbol{\sigma} = \mathbf{C} : \boldsymbol{\varepsilon}^e, \quad (10)$$

$$Q_R = -H^l q, \quad Q^g = l_c^2 H^g \nabla^2 q, \quad (11)$$

being ∇^2 the Laplacian operator.

Regarding a dissipative potential Φ^* , the general non-associated flow rule and the evolution of the internal variable are defined as follows

$$\dot{\boldsymbol{\varepsilon}}^p = \dot{\lambda} \frac{\partial\Phi^*}{\partial\boldsymbol{\sigma}}, \quad \dot{q} = \dot{\lambda} \frac{\partial\Phi^*}{\partial Q_R} \quad (12)$$

where $\dot{\lambda}$ is the rate of the plastic multiplier. To complete the constitutive formulation, the Kuhn-Tucker conditions are introduced

$$\dot{\lambda} \geq 0, \quad \Phi(\boldsymbol{\sigma}, Q_R) \leq 0, \quad \dot{\lambda} \Phi(\boldsymbol{\sigma}, Q_R) = 0 \quad (13)$$

being Φ the yield surface or loading function.

2.1 Gradient-based plastic consistency

Given the loading function Φ , the consistency condition for gradient-based plastic materials leads to

$$\dot{\Phi} = \frac{\partial\Phi}{\partial\boldsymbol{\sigma}} : \dot{\boldsymbol{\sigma}} + \frac{\partial\Phi}{\partial Q_R} \dot{Q}_R. \quad (14)$$

From Eq. (14) and regarding Eqs. (10) to (12), the following differential equation for the plastic multiplier is obtained

$$h \dot{\lambda} + \dot{\Phi}^{trial} + \dot{\Phi}^g = 0, \quad (15)$$

where h is the generalized local plastic modulus. The terms $\dot{\Phi}^{trial}$ and $\dot{\Phi}^g$ are the rates of the local and gradient loading functions, respectively. These values are defined as

$$h = -\frac{\partial\Phi}{\partial\boldsymbol{\sigma}} : \mathbf{C} : \frac{\partial\Phi^*}{\partial\boldsymbol{\sigma}} - H^l \frac{\partial\Phi}{\partial Q_R} \frac{\partial\Phi^*}{\partial Q_R}, \quad (16)$$

$$\dot{\Phi}^{trial} = -\frac{\partial\Phi}{\partial\boldsymbol{\sigma}} : \mathbf{C} : \dot{\boldsymbol{\varepsilon}}, \quad (17)$$

$$\dot{\Phi}^g = l_c^2 H^g \frac{\partial\Phi}{\partial Q_R} \frac{\partial\Phi^*}{\partial Q_R} \nabla^2 \dot{\lambda}. \quad (18)$$

Taking into account Eqs. (12) and (15) and that $\boldsymbol{\varepsilon}^e = \boldsymbol{\varepsilon} - \boldsymbol{\varepsilon}^p$, Eq. (10) can be rewritten as

$$\dot{\boldsymbol{\sigma}} = \mathbf{C}^{ep} : \dot{\boldsymbol{\varepsilon}} + \mathbf{C}^g \dot{\Phi}^g \quad (19)$$

with the fourth-order elastoplastic constitutive tensor

$$\mathbf{C}^{ep} = \mathbf{C} - \frac{1}{h} \left(\mathbf{C} : \frac{\partial\Phi^*}{\partial\boldsymbol{\sigma}} \otimes \frac{\partial\Phi}{\partial\boldsymbol{\sigma}} : \mathbf{C} \right), \quad (20)$$

and the second-order gradient constitutive tensor

$$\mathbf{C}^g = -\frac{1}{h} \mathbf{C} : \frac{\partial\Phi^*}{\partial\boldsymbol{\sigma}}. \quad (21)$$

3 LEON-DRUCKER PRAGER CONSTITUTIVE MODEL EXTENDED FOR RAC (RAC-LDP)

In this section the adopted constitutive equations for RAC are summarized. The Leon-Drucker Prager (LDP) strength criterion originally developed by Vrech and Etse (2009) and extended for RAC (RAC-LDP) by Etse et al. (2016) to account for the recycled aggregate content in the concrete mixture is considered. The RAC-LDP failure criterion, the maximum strength surface in pre- and postpeak regimes and the plastic potential are respectively expressed as

$$\Phi = \frac{3}{2} \beta_R \tau^2 + \gamma_R m_0 \left(\frac{\tau}{\sqrt{6}} + \sigma \right) - c_0 = 0, \quad (22)$$

$$\Phi = \frac{3}{2} \beta_R \tau^2 + \gamma_R m_0 \left(\frac{\tau}{\sqrt{6}} + \sigma \right) - Q_R = 0, \quad (23)$$

$$\Phi^* = \frac{3}{2} \beta_R \tau^2 + \gamma_R m_0 \left(\frac{\tau}{\sqrt{6}} + \eta_R \sigma \right) - Q_R = 0, \quad (24)$$

being σ and τ the Haigh-Westergaard stress coordinates

$$\sigma = \frac{I_1}{3f_c}, \quad \tau = \frac{\sqrt{2J_2}}{f_c}, \quad (25)$$

with f_c the uniaxial compression strength, I_1 the first invariant of the normal stresses and J_2 the second invariant of the deviatoric stresses, while $c_0 = 1$ and $m_0 = 3(f_c^2 - f_t^2) / (2f_c f_t)$.

The influence of the recycled aggregate content is introduced through the parameters β_R and γ_R , computed as

$$\beta_R = \frac{1}{\alpha_R^2} \quad ; \quad \gamma_R = \frac{1}{\alpha_R} \quad (26)$$

which, in turn, are functions of the so-called *concrete mixture recycling factor* α_R , defined as

$$\alpha_R = 1 - \alpha_1 (RA)^{\alpha_2} = \frac{f_c^R}{f_c} \quad \text{being} \quad 0 < \alpha_R \leq 1, \quad (27)$$

where RA is the recycled aggregate ratio and f_c^R is the peak strength in the uniaxial compression test for RAC. The coefficients α_1 and α_2 are positive values to be experimentally calibrated. Moreover, η_R the degree of volumetric non-associativity defined in terms of the confining pressure and recycled aggregate content as

$$\eta_R = \eta - (1 - \eta) \exp [\alpha_R (*\sigma - *\sigma_0) - 1]. \quad (28)$$

Thereby, η is the minimum value of the degree of volumetric non-associativity which is obtained on the edge of the plastic potential, where it intersects the hydrostatic axis. At this stress state the normalized form of the effective first stress coordinate approaches its maximum value $*\sigma = *\sigma_0$.

4 LOCALIZED FAILURE CONDITION OF THE RAC-LDP CONSTITUTIVE MODEL

In quasi-brittle materials like concrete, material failure is characterized by strong spatial discontinuities of the kinematic fields (Willam and Etse (1990), Van Mier (1995)).

In solid continuous, discontinuities may occur in the spatial derivatives of the body velocity $\dot{\boldsymbol{\varepsilon}} = \nabla \dot{\boldsymbol{u}}$. The jump of the kinematic variable can be written as (Hadamard (1903))

$$[[\dot{\boldsymbol{\varepsilon}}]] = [[\nabla \dot{\boldsymbol{u}}]] = \boldsymbol{n} \otimes \boldsymbol{g} \quad (29)$$

being \boldsymbol{n} the normal of the discontinuity surface and \boldsymbol{g} the polarization vector. The balance of the linear momentum across the discontinuity surface leads to the following localization condition (Hadamard (1903))

$$c [[\nabla \cdot \boldsymbol{\sigma}]] + \boldsymbol{n} \cdot [[\dot{\boldsymbol{\sigma}}]] \doteq \mathbf{0}. \quad (30)$$

If a quasi-static problem is considered and neglecting inertial forces, the momentum balance equation yields $\nabla \cdot \boldsymbol{\sigma} = \mathbf{0}$. Finally Eq. (30) implies

$$\boldsymbol{n} \cdot [[\dot{\boldsymbol{\sigma}}]] \doteq \mathbf{0} \quad (31)$$

By considering an homogeneous state before the onset of discontinuous bifurcation, harmonic perturbations are applied to the incremental field variables (displacements and plastic multiplier) which represent the propagation of stationary planar waves. Then, the solutions of the field variables are expressed as

$$\begin{pmatrix} \dot{\boldsymbol{u}} \\ \dot{\lambda} \end{pmatrix} = \begin{pmatrix} \dot{U}(t) \\ \dot{L}(t) \end{pmatrix} \exp \left(\frac{i2\pi}{\delta} \boldsymbol{n} \cdot \boldsymbol{x} \right) \quad (32)$$

being \boldsymbol{x} the position vector and δ the wave length. The spatially homogeneous amplitudes of the wave solutions are represented by $\dot{U}(t)$ and $\dot{L}(t)$. By substituting Eq. (32) into Eq. (18), the following form of the non-local part of the plastic consistency is obtained

$$\dot{\Phi}^g = -h^g \dot{\lambda}, \quad (33)$$

with the generalized gradient modulus computed as

$$h^g = l_c^2 H^g \frac{\partial \Phi}{\partial Q_R} \frac{\partial \Phi^*}{\partial Q_R} \left(\frac{2\pi}{\delta} \right)^2. \quad (34)$$

Taking into account Eqs. (33) and (34), then Eqs. (15) and (19) become

$$(h + h^g) \dot{\lambda} + \dot{\Phi}^{trial} = 0 \quad ; \quad \dot{\boldsymbol{\sigma}} = \mathbf{C}_g^{ep} : \dot{\boldsymbol{\varepsilon}} \quad (35)$$

with

$$\mathbf{C}_g^{ep} = \mathbf{C} - \frac{1}{(h + h^g)} \left(\mathbf{C} : \frac{\partial \Phi^*}{\partial \boldsymbol{\sigma}} \otimes \frac{\partial \Phi}{\partial \boldsymbol{\sigma}} : \mathbf{C} \right). \quad (36)$$

By introducing Eqs. (35-b) and (36) in Eq. (31), the jump of the rate of the Cauchy tensor can be obtained in the non-local form as

$$\mathbf{n} \cdot [[\dot{\boldsymbol{\sigma}}]] = \mathbf{n} \cdot \mathbf{C}_g^{ep} : [[\dot{\boldsymbol{\varepsilon}}]] = \mathbf{Q}_g^{ep} \cdot \mathbf{g} \doteq \mathbf{0} \quad (37)$$

with the second-order gradient acoustic tensor

$$\mathbf{Q}_g^{ep} = \mathbf{Q}^E - \mathbf{n} \cdot \left[\frac{1}{(h + h^g)} \left(\mathbf{C} : \frac{\partial \Phi^*}{\partial \boldsymbol{\sigma}} \otimes \frac{\partial \Phi}{\partial \boldsymbol{\sigma}} : \mathbf{C} \right) \right] \cdot \mathbf{n} \quad (38)$$

where $\mathbf{Q}^E = \mathbf{n} \cdot \mathbf{C} \cdot \mathbf{n}$ is the second-order elastic acoustic tensor. Finally, localization of deformation takes place if Eq. (37) admits a solution for any polarization vector \mathbf{g} different to zero. Consequently, the following condition must be fulfilled

$$\det(\mathbf{Q}_g^{ep}) = 0. \quad (39)$$

Note that in case of local materials Eq. (38) becomes

$$\mathbf{Q}^{ep} = \mathbf{Q}^E - \mathbf{n} \cdot \left[\frac{1}{h} \left(\mathbf{C} : \frac{\partial \Phi^*}{\partial \boldsymbol{\sigma}} \otimes \frac{\partial \Phi}{\partial \boldsymbol{\sigma}} : \mathbf{C} \right) \right] \cdot \mathbf{n} \quad (40)$$

and therefore, the localization condition leads to

$$\det(\mathbf{Q}^{ep}) = 0. \quad (41)$$

Note that the above equations are affected by the recycled aggregate content by means of the dependency of Φ and Φ^* on RA .

5 NUMERICAL ANALYSIS OF THE LOCALIZED FAILURE WITH THE THE RAC-LDP MODEL

In this section, the transition point from ductile to brittle failure mode is analyzed regarding plane stress and plane strain conditions. For this localization analysis, the concrete properties by Folino and Xargay (2014) and the model parameters listed in Table (1) are used.

The performance of the localized failure indicator is evaluated on the maximum strength surface of the gradient and fracture energy based model for RAC. The variation of the normalized localization indicators $\det(\mathbf{Q}_g^{ep})/\det(\mathbf{Q}^E)$ and $\det(\mathbf{Q}^{ep})/\det(\mathbf{Q}^E)$ are shown along the maximal strength criterion defined in terms of the normalized principal stresses (σ_1/f_c ; σ_2/f_c) for four different recycled aggregate contents: $RA = 0, 0.30, 0.60$ and 1 , for plane stress and strain

E	31.67 GPa
f_c	36.52 MPa
f_t	4.04 MPa
α_{r1}	0.00075
α_{r2}	1.25
η_0	0.30

Table 1: Concretes properties.

conditions, see Figs. (1) and (2), respectively. The normalized localization indicator is represented as an ordinate in the normal direction to the corresponding maximum strength surface. Positive values are shown in the outward direction. The intersections between the maximum strength surfaces and the envelope of the segments representing the norm of the localization tensor signalizes the so-called transition point (TP) from ductile to brittle failure mode.

According to the results in Fig. (1), it can be concluded that under plane stress conditions, the material failure modes show very low dependency on the recycled aggregate content. This fact follows from the comparison between the length of the zones under localized failure with respect to the total perimeter of the failure surface, for each particular recycled aggregate content. This ratio remains practically invariant with the different recycled aggregate content. However, this conclusion does not mean that the critical direction for localization is independent of the recycled aggregate content.

Regarding Fig. (2), corresponding to plane strain conditions, it can be concluded that for lower recycled aggregate contents, the material behaves very stable in almost all the stress domain and there is evidence of discontinuous bifurcation only very close to the apex, while for higher recycled aggregate contents, localized failure modes are a little bit more evident. In contrast to the plane stress state, the transitions points only appear in zones of very low confinement, while in plane stress conditions there is evidence of discontinuous bifurcation also in high confinement regimes. This means that the plane strain condition as compare to the plane stress one is related to more stable failure modes all along the failure surface.

6 CONCLUSIONS

Thermodynamically consistent gradient-based constitutive theory extended to simulate the failure behavior of RAC composed by arbitrary recycled aggregate contents is able to capture the influence of the recycled aggregate content on the failure response behavior. In this regard, the analysis of the localization indicator, in terms of the determinant to the localization tensor, have been performed at peak stress of plane stress and strain states. Under plane stress conditions, the material failure modes show very low dependency on the recycled aggregate content, while under plane strain conditions and higher recycled aggregate contents, localized failure modes are a little bit more evident. In contrast to the plane stress state, in plane strain state the transitions points only appear in zones of very low confinement. This means that the plane strain condition as compare to the plane stress one is related to more stable failure modes all along the failure surface.

REFERENCES

- Du T., Wang W., Liu Z., Lin H., and Guo T. The complete stress-strain curve of recycled aggregate concrete under uniaxial compression loading. *J. of Wuhan University of Technology Mater.*, 25(5):862–865, 2010.
- Etse G., Vrech S., and Ripani M. Constitutive theory for recycled aggregate concretes subjected

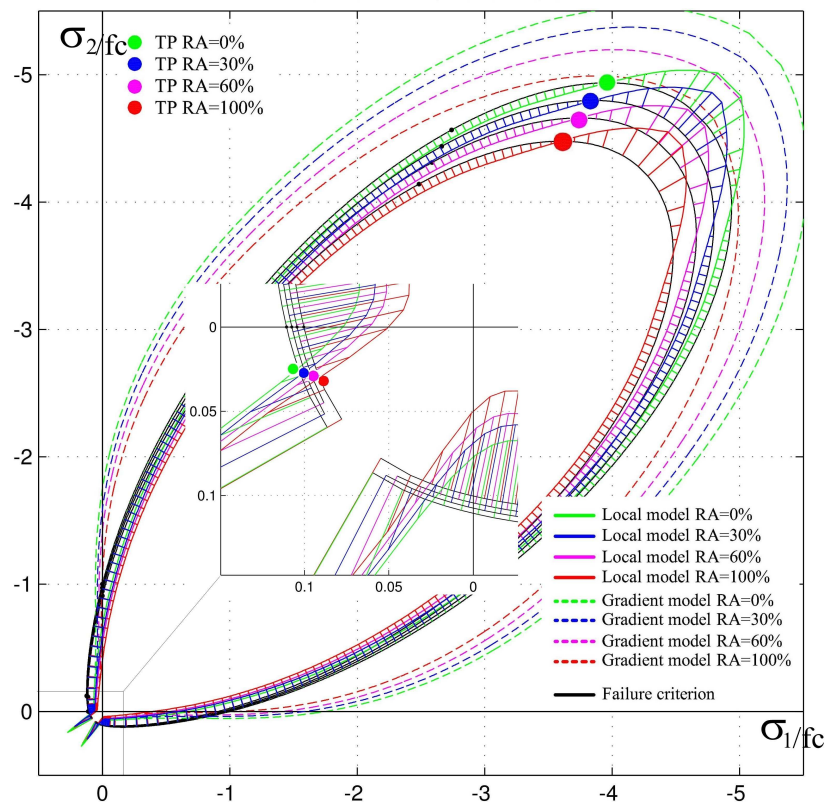


Figure 1: Normalized localization indicators drawn in normal direction to the RAC-LDP maximum strength criterion under plane stress state.

to high temperature. *Const. and Build. Mat.*, 111:43–53, 2016.

Folino P. and Xargay H. Recycled aggregate concrete-mechanical behavior under uniaxial and triaxial compression. *Constr. Build. Mater.*, 56:21–31, 2014.

Hadamard J. Propagation des ondes et les équations de l'hydrodynamique. *Int. J. for Num. Meth. in Eng.*, 35:69–76, 1903.

Kou S. and Poon C. Enhancing the durability properties of concrete prepared with coarse recycled aggregate. *Constr. Build. Mater.*, 35:69–76, 2012.

Li J., Xiao J., and Huang J. Microplane model for recycled aggregate concrete. *Proc. 2nd International Conference on Waste Engineering and Management, ICWEM, Shanghai, China*, pages 542–550, 2010.

Lima C., Caggiano A., Faella C., Martinelli E., Pepe M., and Realfonzo R. Physical properties and mechanical behaviour of concrete made with recycled aggregates and fly ash. *Constr. Build. Mater.*, 47:547–559, 2013.

NRMCA. *Concrete CO₂ Fact Sheet*, volume 13. National Ready Mixed Concrete Association. Silver Spring, MD, www.nrmca.org, 2012.

NTC. *Italian Recommendations, Decreto Ministeriale: 14 gennaio*, volume 19. 2008.

RILEM-TC-121-DRG. *Specifications for concrete with recycled aggregates*, volume 27. Mater. Struct., 1994.

Simo J. and Miehe C. Associative coupled thermoplasticity at finite strains: formulation, numerical analysis and implementation. *Comput. Meth. Appl. Mech.*, 98:41–104, 1992.

Svedberg T. and Runesson K. A thermodynamically consistent theory of gradient-regularized

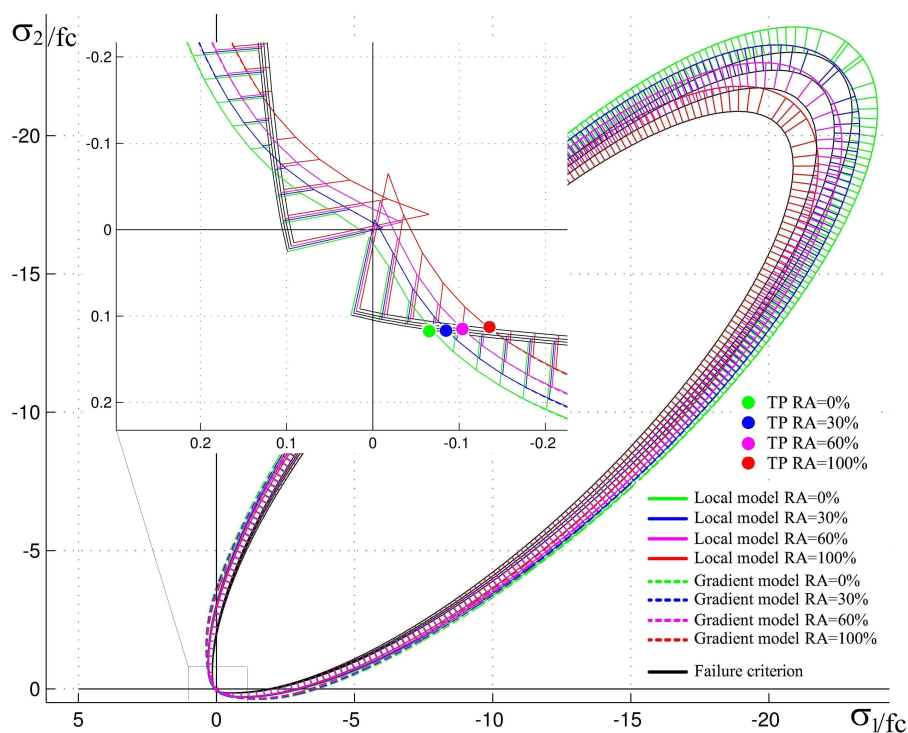


Figure 2: Normalized localization indicators drawn in normal direction to the extended LDP maximum strength criterion under plane strain state.

plasticity coupled to damage. *Int. J. Plasticity*, 13(6-7):669–696, 1997.

Van Mier J.G.M. *Fracture processes of concrete*. CRC Press, U.S., 1995.

Vrech S. and Etse G. Gradient and fracture energy-based plasticity theory for quasi-brittle materials like concrete. *Comput. Meth. Appl. Mech.*, 199(1-4):136–147, 2009.

Willam K. and Etse G. Failure assessment of the extended Leon model for plain concrete. *Proc. SCI-C Conf., Zell and See, Austria, Pineridge Press, Swansea, UK*, 13(6-7):851–870, 1990.